PETROVIETNAM JOURNAL
Volume 6/2019, p. 4 - 15
ISSN-0866-854X

Influence of rock physics parameters on construction of rock physics template for Middle Miocene sand in Nam Con Son basin

Pham Huy Giao[1], Mai Thi Huyen Trang[1, 2] and Pham Hong Trang[1, 2]
[1]Asian Institute of Technology
[2]Vietnam Petroleum Institute
Email: hgiao@ait.asia

Summary

Rock physics template (RPT) is a relative new tool of reservoir characterisation that can aid interpretation of well log data to help reduce the risks in seismic exploration and prospect evaluation. One of the popular RPTs is the crossplot of V_p/V_s (Compressional wave velocity/Shear wave velocity) versus AI (acoustic impedance) that proved to be very successful in reservoir characterisation of shallow unconsolidated sediments in the North Sea. However, construction of a RPT is very site dependent, thus when one extends the application of this type of RPT to other sites for those reservoirs that might be located deeper or consist of more consolidated or cemented sediments an adequate attention has to be given to the parameters in the rock physics models that are at the foundation of a RPT construction. This study deals with construction of a new RPT for the Middle Miocene sand (MMS), a gas-bearing sand located around 3,500m TVDSS (True vertical depth subsea) at Hai Thach field, Nam Con Son basin. In this research an emphasis was given to study the influence of elastic bounds and rock physics parameters such as critical porosity, coordination number, mineral fraction, dry bulk and shear moduli on construction of the RPT. As results a new RPT was successfully constructed using the Voigt-Reuss-Hill elastic bound and modified Gassmann's equation for the gas-bearing Middle Miocene Sand, which could be characterised with acoustic impedance (AI) from 9,000 to 11,000 m/s×g/cc, V_p/V_s from 1.65 to 1.8, porosity from 11 to 16%, and gas saturation from 50% up.

Key words: Nam Con Son basin, gas sand, rock physics model (RPM), rock physics template (RPT), elastic bound, Gassmann's equation.

1. Introduction

It is well known that hydrocarbon in Vietnam has been mainly produced from the fractured granite basement reservoirs, in particular in the Cuu Long basin. This trend has gradually changed and the contributions from clastic reservoirs become more and more important as illustrated in Figure 1. Characterisation of clastic sands in various petroleum basins is therefore a task of primary importance of exploration and production sector in the years ahead.

In this study, construction of a rock physics template (RPT), a relatively new tool but quite commonly used at the moment for petrophysical characterisation of a clastic reservoir, is presented in detail for MMS, a gas bearing turbidite sands in Hai Thach field of the Nam Con Son basin. As a matter of fact the properties of MMS are relatively

Date of receipt: 3/5/2019. Date of review and editing: 3/5 - 2/7/2019.
Date of approval: 3/7/2019.

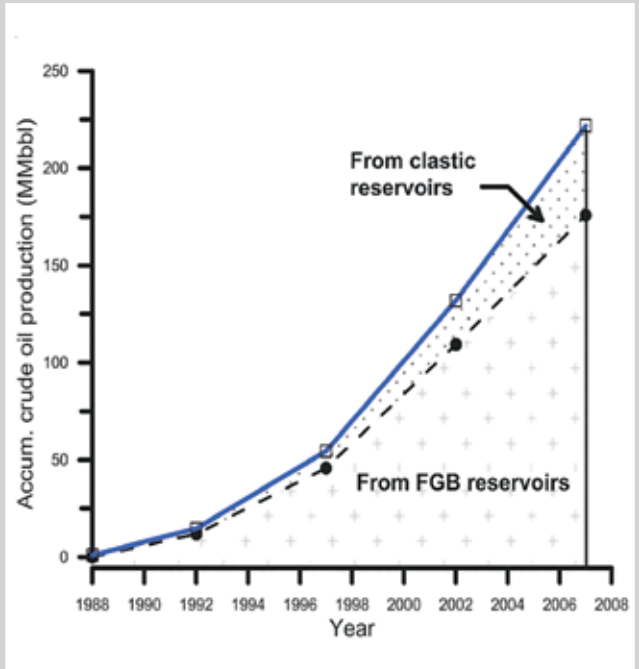

Figure 1. *Petroleum production trends in Vietnam from 1988 to 2008 [1].*

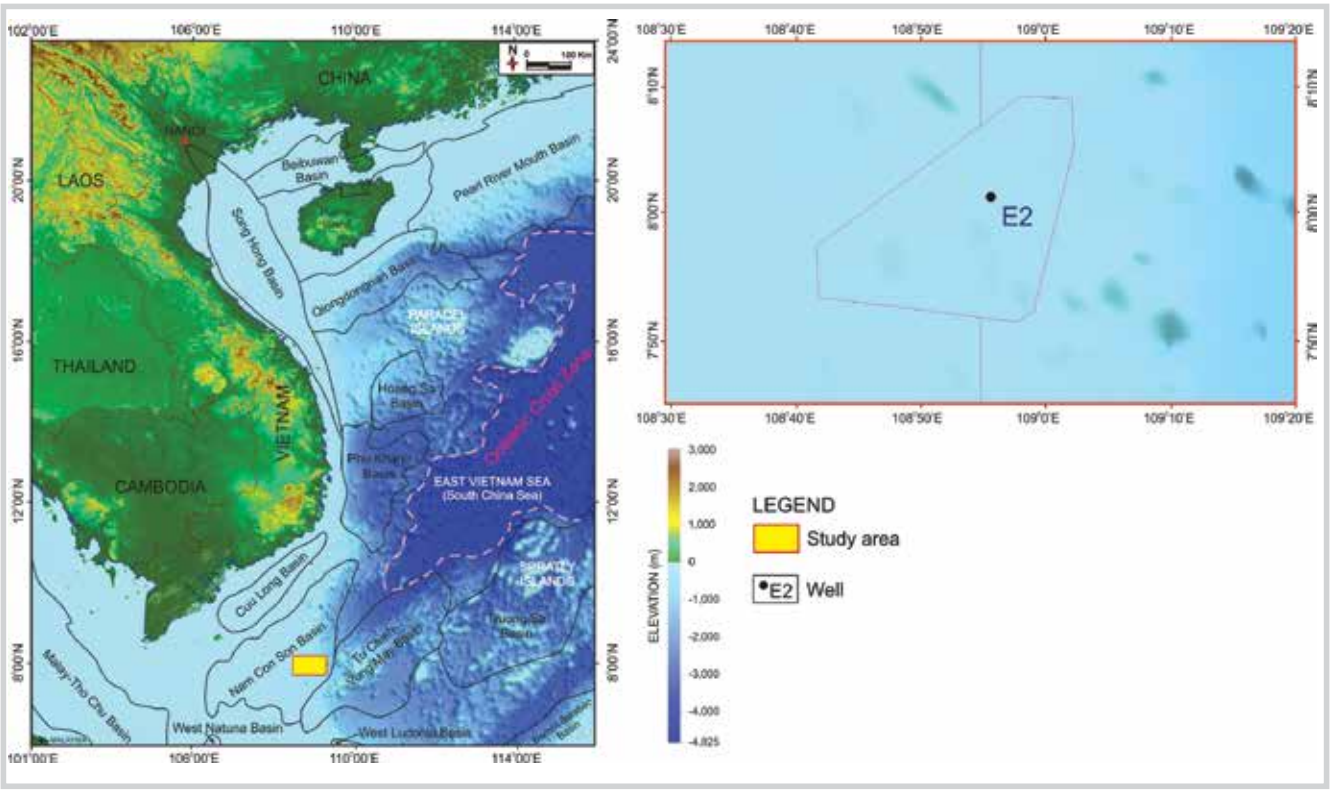

Figure 2. *Nam Con Son basin (left inset) and the study well location (right inset) [2].*

difficult to be identified on the conventional seismic data and post-stack inversion results owing to their complex lithology with appearance of calcite veins that would probably cause an increase in acoustic impedance (AI) of this sand. The objective of this study is to investigate the influences of rock physics parameters on construction of a RPT for MMS and propose a systematic procedure to apply it, taking into account the site-specific conditions of the study location.

2. Middle Miocene sand in Nam Con Son basin

The Nam Con Son basin lies on the continental shelf margin, offshore Vietnam. The basin type is of Cenozoic rift and regional subsidence [3]. It is bounded to the southwest by the Con Son swell and Khorat - Natuna arch, and to the west by the Tu Chinh - Vung May basin (Figure 2). The geological evolution of the Nam Con Son basin is closely related to the East Sea spreading and can be divided into main stages, i.e., syn-rift 1, inter-rift, syn-rift 2 and post-rift [2, 4, 5]. A seismic cross-section in Figure 3 shows geological sequences of the Nam Con Son basin consisting of Pre-Tertiary basement, Early Oligocene (T10), Late Oligocene (T20), Early Miocene (T30), Middle Miocene (T40, T50, T60, T65), and Late Miocene (T85). Rifting in Nam Con Son basin started during the Late Eocene to Early Oligocene, which was followed by seafloor spreading in the East Sea between the end of the Early Oligocene (32Ma) and the start of the Middle Miocene (15Ma) when it is characterised by thermal subsidence (sag phase) and widespread deposition of a thick package up to 2,000m of fluvial deltaic sediments. This sequence (T20 - T30) includes the paralic coals that are the main source rock of the basin petroleum system. Seafloor spreading in the East Sea stopped around 15Ma and was followed by a renewed rifting during the Middle Miocene. This phase propagated from North East to South West and is responsible for the structure and trap formation in the basin. The end of the Mid Miocene rifting event is marked by a pronounced unconformity (Middle Miocene unconformity), followed by the deposition of a thick post-rift ("sag phase") wedge, which includes the massive Plio-Pleistocene proto-Mekong shelf edge delta system, prograding from West to East. The rapid deposition of this package caused over-pressuring in the central basin, concentrated in a SSW-NNE oriented belt where the post-rift wedge is the thickest. The major discovery and production of hydrocarbons in the formations of basement, clastics and carbonates with age ranging from Pre-Cenozoic to Miocene are marked in the stratigraphic column of the Nam Con Son basin in Figure 4.

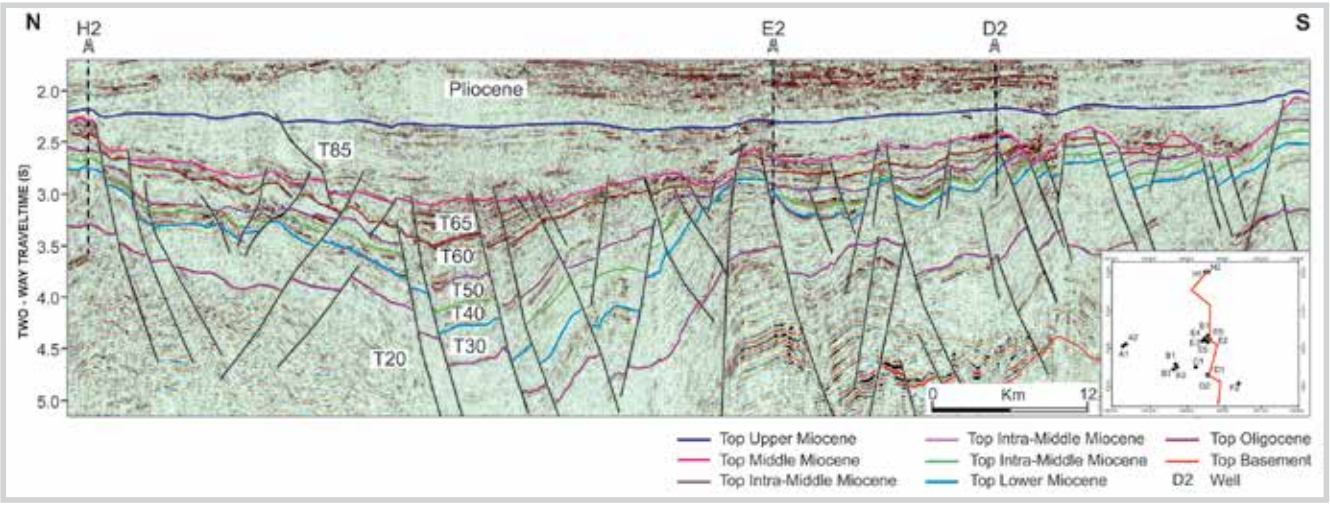

Figure 3. *A seismic section of the Nam Con Son basin [2].*

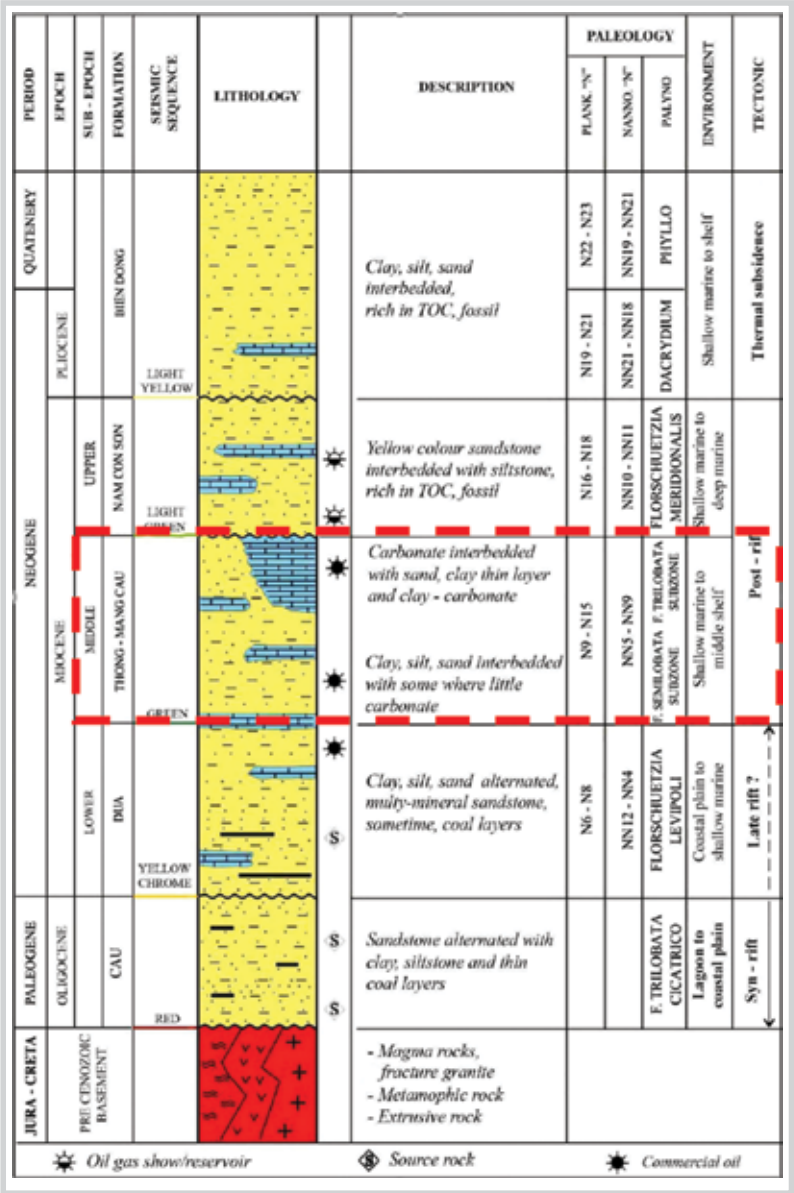

Figure 4. *Stratigraphic column of the Nam Con Son basin [6].*

Hai Thach field: The exploration and production activities in the Nam Con Son basin have led to discovery of many fields in various stratigraphic sequences including fractured basement (e.g. Dai Hung, Gau Chua), Oligocene (e.g. Rong Doi, Ca Rong Do), Lower Miocene (e.g. Rong Vi Dai, Ca Rong Do), Middle Miocene (e.g. Chim Sao, Dua, Dai Nguyet, Thien Ung, Mang Cau), Upper Miocene (e.g. Hai Thach, Moc Tinh, Lan Tay, Lan Do). Hai Thach field was discovered in 1995 by a BP (British Petroleum) exploration well drilled right on the Hai Thach horst structure, in which gas and condensate accumulations were found from multiple stacked reservoir units in Miocene, i.e. UMA10 (Upper Miocene), MMH10 (Mid Miocene), LMH10, LMH20 and LMH30 (Lower Miocene). Another BP well drilled on the eastern flank of the Hai Thach structure encountered additional HC-bearing sandstones in Upper Miocene (UMA15) and Middle Miocene (MMF10, MMF15 and MMF30). The appraisal and production wells confirmed gas and condensate presence in the MMF30 interval, which is the very target sand reservoir for RPT construction in this study as explained more in details in the following.

The Middle Miocene sand (MMS) belongs to the Thong - Mang Cau formation (Middle Miocene), which is widely distributed in the Nam Con Son basin and

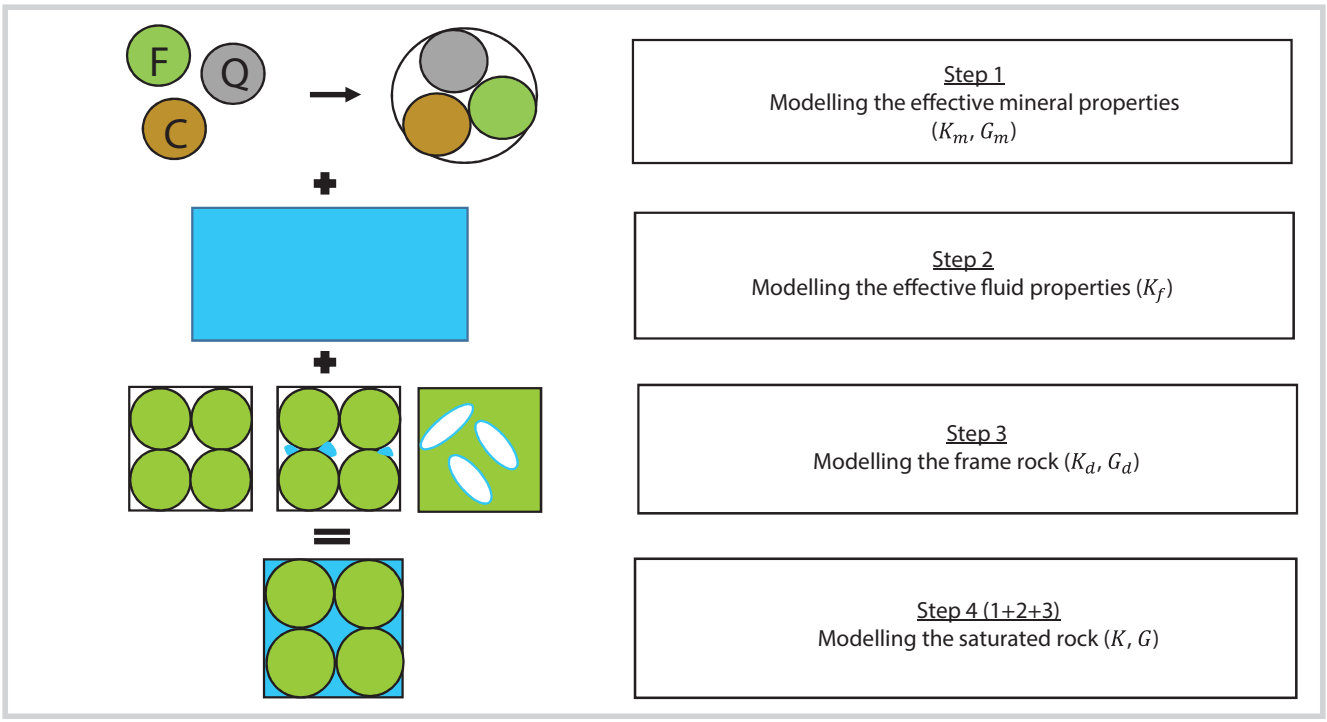

Figure 5. *Rock physics modelling process (modified from [7]).*

consists of two main parts, i.e. the lower part, mainly composed of fine to medium-grained quartz sandstone with carbonate cement, rich in glauconite and marine fossils interbedded with thin layers of claystone and carbonaceous shale; and the upper part, dominated with intercalation of light grey and milky white or sometimes reddish brown dolomitised carbonate and layers of greenish grey shale-siltstone, and fine-grained sandstone containing carbonate cement. Middle Miocene sediments were accumulated predominantly in open marine, outer shelf to bathyal depositional environments. On the flank area, reservoir quality is quite different from well to well. The sediments of reservoir interval (MMF30) were deposited as turbidites/slumps in the deep marine environment and have reservoir quality from fair to good, with average porosity from 14 to 16% and a net thickness from 25 to 43m TVD (True vertical depth). The resistivity readings show significant offset from the background, i.e., 10 to 20Ωm versus 2.0Ωm.

3. Rock physics model (RPM) and rock physics template (RPT)

3.1. Rock physics model (RPM)

A rock physics model is a mathematical relation between elastic and intrinsic properties of a rock such as mineralogy, grain and pore geometry, porosity and connectivity. Rock physics modelling is the process to

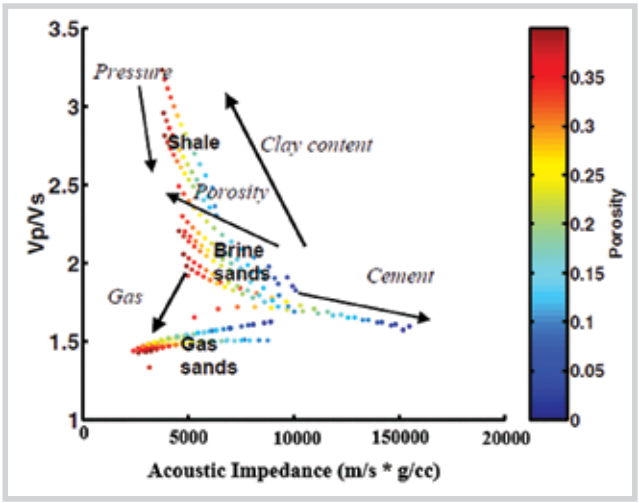

Figure 6. *RPT for North Sea Sand [8].*

estimate bulk and shear moduli of mineral components, pore fluids, and rock frame, following the steps as shown in Figure 5. Some typical rock physics models that are commonly used in developing the rock physics templates can be seen in Equations 1 - 3.

3.2. Rock physics template (RPT)

Any chart or cross-plot between two types of elastic or geomechanical parameters based on which one can figure out the reservoir properties of interest such as lithology and fluid type, shale content, cementing type, porosity, permeability, hydrocarbon saturation, etc. can

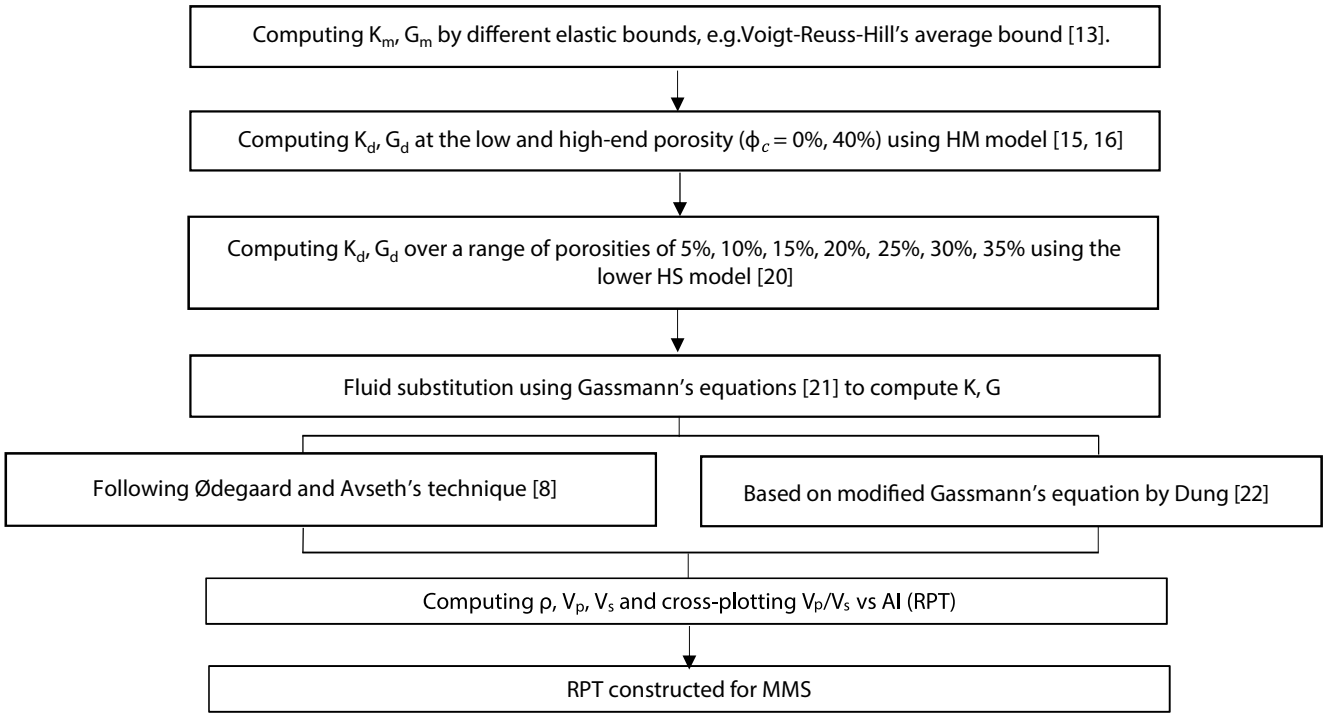

Figure 7. *Flow chart of the study.*

be considered as a rock physics template (RPT). One of the most popular RPTs at the moment is that proposed by [8] for North Sea Sand based on rock physics model of [9]. This RPT is a crossplot of V_p/V_s versus acoustic impedance (AI) of P-wave and can be used to estimate rock and fluid types of a reservoir as presented in Figure 6. Ødegaard and Avseth stated that "the rock physics templates provide an important interpretation tool that can improve communication between geologists and geophysicists and can help reduce risk in seismic exploration and prospect evaluation" [8]. The often-encountered problem in application of this technique is that the practical engineers tend to pay little attention to parameters involved in the rock physics models that are foundations for construction of RPT, ignoring their effects, and consequently the well data could not match with the RPT they constructed for the study site. It was made clearly that "a rock physics model should never be considered to be universal, but should be site specific and honor local geological factors. Geological constraints on rock physics models include lithology, mineralogy, burial depth, diagenesis, pressure and temperature. All these factors must be considered when generating rock physics templates for a given basin" [8]. In this study, the technique [8] was slightly modified to consider better the site conditions of Hai Thach field for construction of RPT for MMS as explained more in detail in the following sections.

4. Methodology

The flowchart to construct the RPT in this research follows that conducted by [10] as shown in Figure 7. In the first step, the bulk and shear mineral moduli (K_m, G_m) are calculated using one of the rock physic models shown in Equations 1a-d, known as the elastic bounds and plotted in Figure 8. To have properly calculated mineral moduli the fractions of each rock-forming constituent mineral are desired to be known, which are usually identified by the XRD (X-Ray Diffraction) analysis results as seen in Table 1a for the MMS core samples from the study well E2, Table 1b shows the moduli of some typical constituent minerals of a sandstone.

Voigt (1910) $$K_m = \sum_{i=1}^{N} f_i K_i \quad (1a)$$

$$G_m = \sum_{i=1}^{N} f_i G_i \quad (1b)$$

Reuss (1929) $$\frac{1}{K_m} = \sum_{i=1}^{N} \frac{f_i}{K_i} \quad (1c)$$

$$\frac{1}{G_m} = \sum_{i=1}^{N} \frac{f_i}{G_i} \quad (1d)$$

Hill (1952) $$K_m = \frac{1}{2}\left[\sum_{i=1}^{m} f_i K_i + \left(\sum_{i=1}^{m} \frac{f_i}{K_i}\right)^{-1}\right] \quad (1e)$$

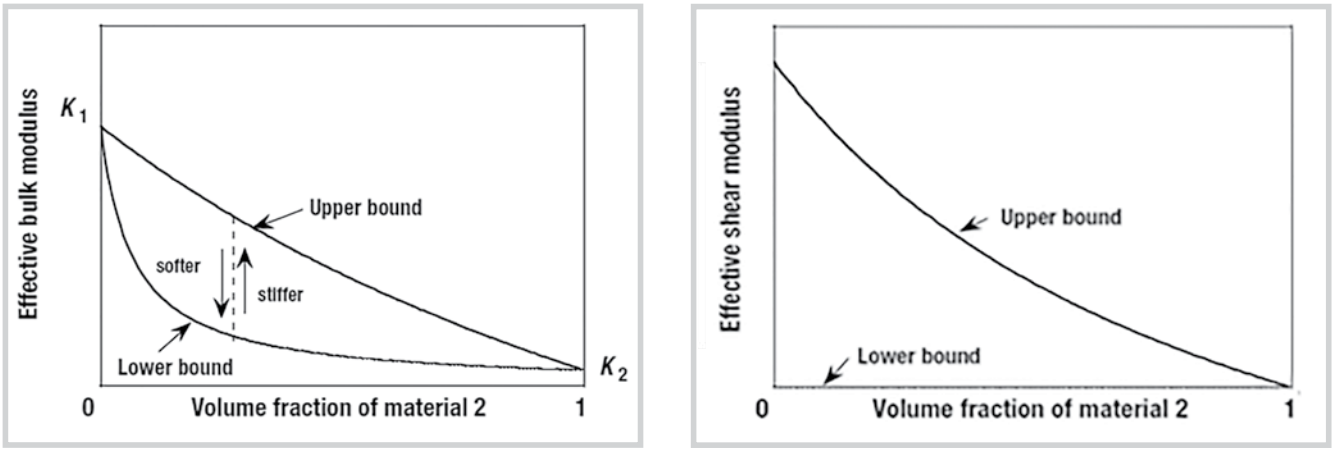

Figure 8. *The upper and lower elastic bounds: the upper bound in Equations 1a-b [11], the lower bound in Equations 1c-d [12] and the Voigt-Reuss-Hill average bound in Equations 1e-f [13].*

Table 1a. *Results of XRD analysis of some cores from the well E2*

Depth (m)	Quartz	Mica-clay	K-Feldspar	Plagioclase	Calcite	Dolomite	Siderite	Pyrite
3587.35	66	5.5	12	12	0.5	1.5	2.5	
3591.65	86.5	1	5.5	5.5	0.5		1	
3598.25	86.5	1	5.5	6				1
3601.25	85	2.5	4.5	7			1	
3610.35	68	5.5	6	9		3	8.5	
3612.35	72.5	7.5	5	10.5	0.5	2.5	1.5	
Percent (%)	77.42	3.83	6.42	8.33	0.5	2.33	2.9	1

Table 1b. *Moduli of some typical minerals [14]*

Mineral type	Quartz	Mica-clay	K-Feldspar	Plagioclase	Calcite	Dolomite	Siderite	Pyrite
Bulk moduli (GPa)	36.6	21	75.6	55	76.8	94.9	123.7	147.4
Shear moduli (GPa)	45	7	25.6	28	32	45	51	132.5
Density (g/cc)	2.65	2.58	2.62	2.56	2.71	2.87	3.96	4.93

$$G_m = \frac{1}{2}\left[\sum_{i=1}^{m} f_i G_i + \left(\sum_{i=1}^{m} \frac{f_i}{G_i}\right)^{-1}\right] \quad (1f)$$

Where: f_i, K_i, and G_i are the volume fraction, bulk modulus and shear modulus of the i^{th} constituent mineral, respectively; K_m, G_m are bulk and shear moduli of the rock matrix.

In the second step, the elastic moduli of the dry rock frame (K_d, G_d) are calculated using Hertz-Mindlin's model [15, 16] (also known as the HM model) for the low and high-end porosity corresponding to ϕ = 0% and 40%, respectively, based on Equations 2a-b:

$$K_{HM} = \left[\frac{n^2(1-\phi_c)^2 G_m^{\,2}}{18\pi^2(1-\nu_m)^2} P\right]^{\frac{1}{3}} \quad (2a)$$

$$G_{HM} = \frac{5-4\nu_m}{5(2-\nu_m)}\left[\frac{3n^2(1-\phi_c)^2 G_m^{\,2}}{2\pi^2(1-\nu_m)^2} P\right]^{\frac{1}{3}} \quad (2b)$$

$$\nu_m = \frac{3K_m - 2G_m}{2(3K_m + G_m)} \quad (2c)$$

$$P = g\int_0^Z (\rho_b - \rho_f)\, dz \quad (2d)$$

$$n = 20 - 34\phi + 14\phi^2 \quad (2e)$$

Where the critical porosity (ϕ_c) is an important parameter that is defined as the porosity above which the rock can exist only as a suspension. In this case the grains are not in contact anymore and are suspended in water and the stiffness of the sediment is determined by the pore fluid. Below the critical porosity, the stiffness of the rock is determined by the framework of contacting mineral grains. In sandstone critical porosity varies from 36% to 40%, and that is porosity of a random close pack of well-sorted rounded quartz grains. This is often the starting point for the formation of consolidated sandstones. In our study for MMS the critical porosity of 40% was used for calculation of K_d and G_d by Equations 2a-b. The critical porosity of different rock types may differ between them as seen in Table 2. Another important parameter in rock physics model is the co-ordination number or contact number (n), which is defined as the average number

Table 2. *Critical porosity of some rock types [19]*

Rock type	Critical Porosity (%)
Sandstones	40
Limestones	40
Dolomites	40
Pumice	80
Chalks	65
Rock salt	40
Cracked igneous rocks	5
Oceanic basalt	20
Sintered glass beads	40
Glass foam	90

of contacts per grain [14]. The contact number can be estimated by empirical relationships proposed by [17] or [18]. In this study, for the final RPT n was chosen equal to 8.64 corresponding to ϕ_c = 40%. The mineral Poisson's ratio (ν_m) is related to K_m and G_m as seen in Equation 2c. P is the effective pressure at the depth level of the target reservoir. ρ_b, ρ_f are bulk density and fluid density in g/cc, respectively, g is the gravitational acceleration equal to 9.81m/s^2, and z is the depth (m).

The next step in constructing the RPT is to calculate K_d and G_d for the range of porosities between two end values of 0% and critical porosity, say, ϕ = 5%, 10%, 15%, 20%, 25%, 30%, 35% using Equations 3a-c, which are Hashin-Shtrikman's model [20] or shortly known as the HS model:

$$K_d = \left[\frac{\frac{\phi}{\phi_c}}{K_{HM} + \frac{4}{3}G_{HM}} + \frac{1 - \frac{\phi}{\phi_c}}{K_m + \frac{4}{3}G_{HM}}\right]^{-1} \quad (3a)$$

$$G_d = \left[\frac{\frac{\phi}{\phi_c}}{G_{HM} + Z} + \frac{1 - \frac{\phi}{\phi_c}}{G_m + Z}\right]^{-1} - z \quad (3b)$$

$$z = \frac{G_{HM}}{6}\left[\frac{9K_{HM} + 8G_{HM}}{K_{HM} + 2G_{HM}}\right] \quad (3c)$$

In the 4th step, fluid substitution was conducted to calculate the saturated moduli (K, G) by Gassmann's equations [21] starting with Equations 4 - 5 below. In addition, the fluid bulk modulus (K_f) was calculated by Equation 6 following Reuss's lower elastic bound [12]:

$$\frac{K}{K_m - K} = \frac{K_d}{K_m - K_d} + \frac{K_f}{\phi(K_m - K_f)} \quad (4)$$

$$G = G_d \quad (5)$$

$$\kappa_f = \left[\frac{S_w}{K_w} + \frac{1-S_w}{K_{hc}}\right]^{-1} \quad (6)$$

Once the elastic moduli are known, the elastic wave velocities are determined based on Equations 7 - 10, and finally a cross plot between V_p/V_s and AI can be constructed.

$$V_p = \sqrt{\frac{K + 4/3G}{\rho_b}} \quad (7)$$

$$V_s = \sqrt{\frac{G}{\rho_b}} \quad (8)$$

$$\rho_s = (1-\phi)\rho_m + \phi\left[(1-S_w)\rho_g + S_w\rho_w\right] \quad (9)$$

$$AI = \rho_b V_p \quad (10)$$

Where: V_p, V_s are the saturated compressional and shear wave velocity (m/s), respectively; AI is acoustic impedance m/s×g/cc); ρ_s, ρ_m, ρ_w, ρ_g, are saturated density, matrix density, water density and gas density, respectively.

Regarding the calculation of mineral moduli using HM model (Equations 1a-f), both mono-mineral and multi mineral cases were studied. For the former case with Quartz being the only constituent mineral the input parameters used for calculation are shown in Table 3, while for the latter case K_m and G_m were determined based on the mineral fractions identified by the XRD analysis as shown in Table 1a.

Table 3. *Input parameters for the mono-mineral case with Quartz being the only constituent mineral*

Critical porosity ø = 40%	K_m = 36.6GPa
Coordinate number n = 8.64	G_m = 45GPa
Effective pressure P = 0.057GPa @ 3,548m TVDSS	ρ = 2.65g/cc

Notably, as indicated in Figure 7, to take into account the site-specific conditions of Hai Thach field, calculation of the dry modulus (K_d) in the second step can be done using a modified form of Gassmann's equation proposed by [22] as shown in Equations 11a-b. In this approach, the petrophysical parameters such as K, G, K_f, porosity were directly determined from well log analysis of the study well and introduced into Equation 11a to calculate the Biot coefficient (α), based on which K_d can be determined using Equation 11b as follows:

$$\left[\phi(K_m - K_f) - K_f\left(1 - \frac{K}{K_m}\right)\right]\alpha = \phi\left[\left(K_m - K_f\right) - K\left(1 - \frac{K_f}{K_m}\right)\right] \quad (11a)$$

$$\alpha = 1 - \frac{K_d}{K_m} \quad (11b)$$

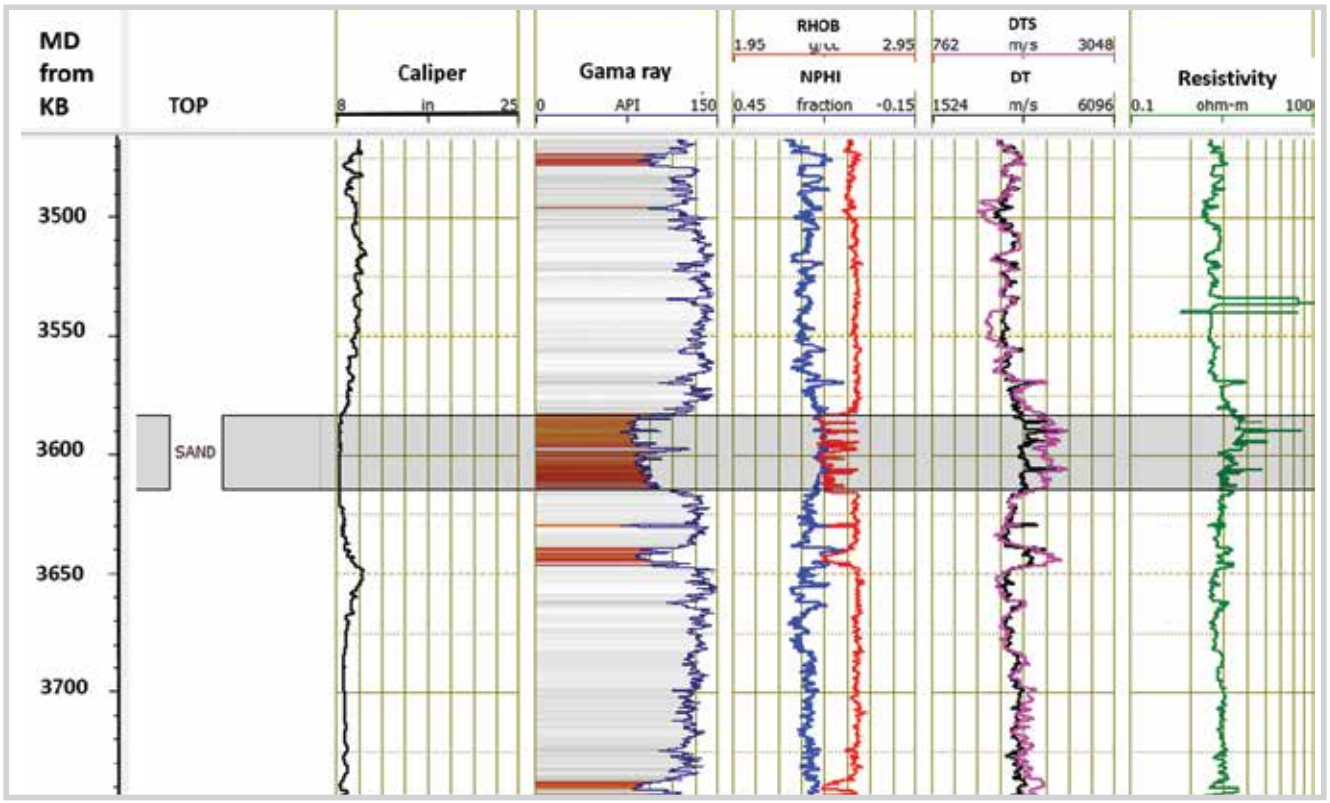

Figure 9. *The MMS reservoir interval from 3,548.57 to 3,584.40m TVDSS, E2 well.*

Table 4. *The rock physics parameters used for estimation of K_d and G_d*

Porosity = 0.14	Matrix	Dry rock frame
Effective pressure = 0.033 GPa	K_m = 36.52 GPa	K_d = 21.91 GPa
	G_m = 31.64 GPa	G_d = 12 GPa

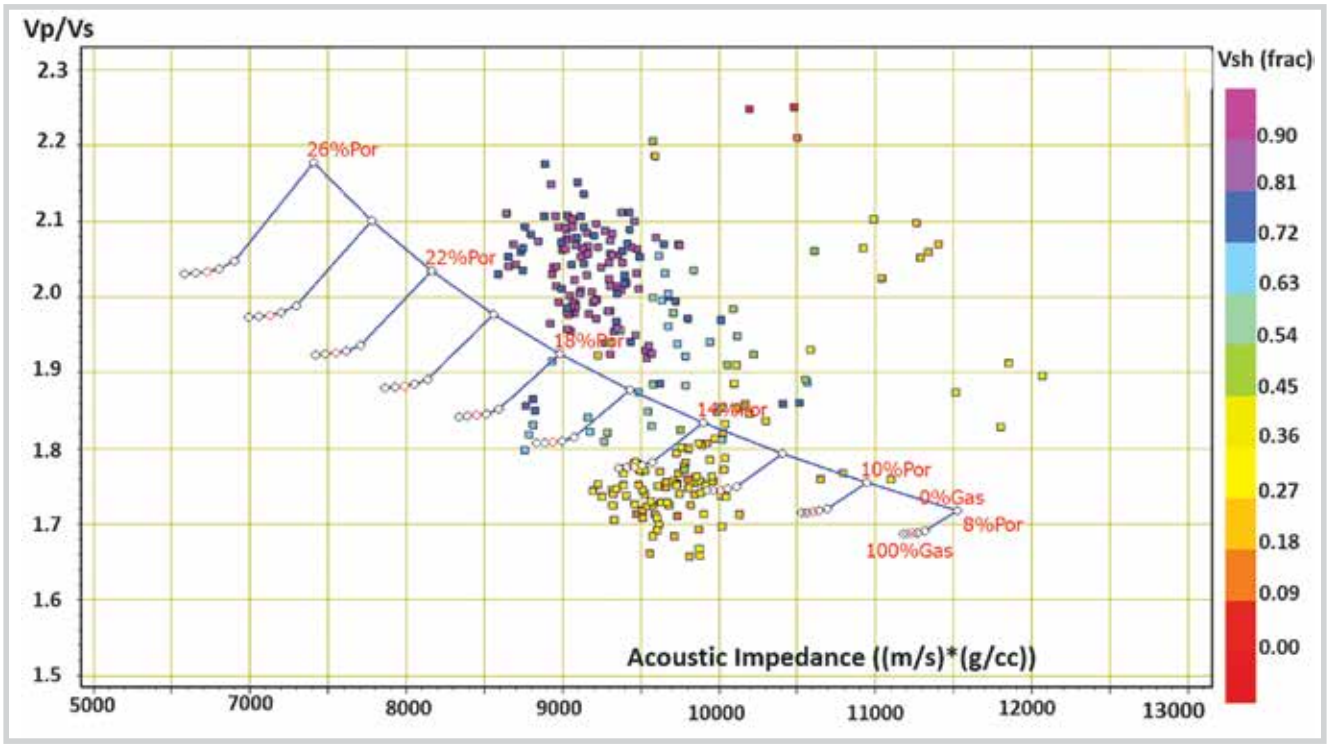

Figure 10. *The RPT constructed for MMS method using Hampson-Russel software.*

5. Results and discussions

5.1. Construction of RPT using Hampson-Russel software

Geoview is the main tool in HR (Hampson-Russell) software that can be used to analyse data and construct RPT. First, the well-log data of CAL (Caliper), GR (Gamma Ray), RHOB (Bulk density), NPHI (Neutron porosity), LLD (Depth resistivity), DT (Compressional wave slowness), DTS (Shear wave slowness) are loaded into Geoview through Data Explorer (Figure 9). The MMS has low GR from 80 to 90API (American Petroleum Institute), LLD from 3 to 10Ωm, NPHI from 0.09 to 0.18, RHOB from 2.42 to 2.65

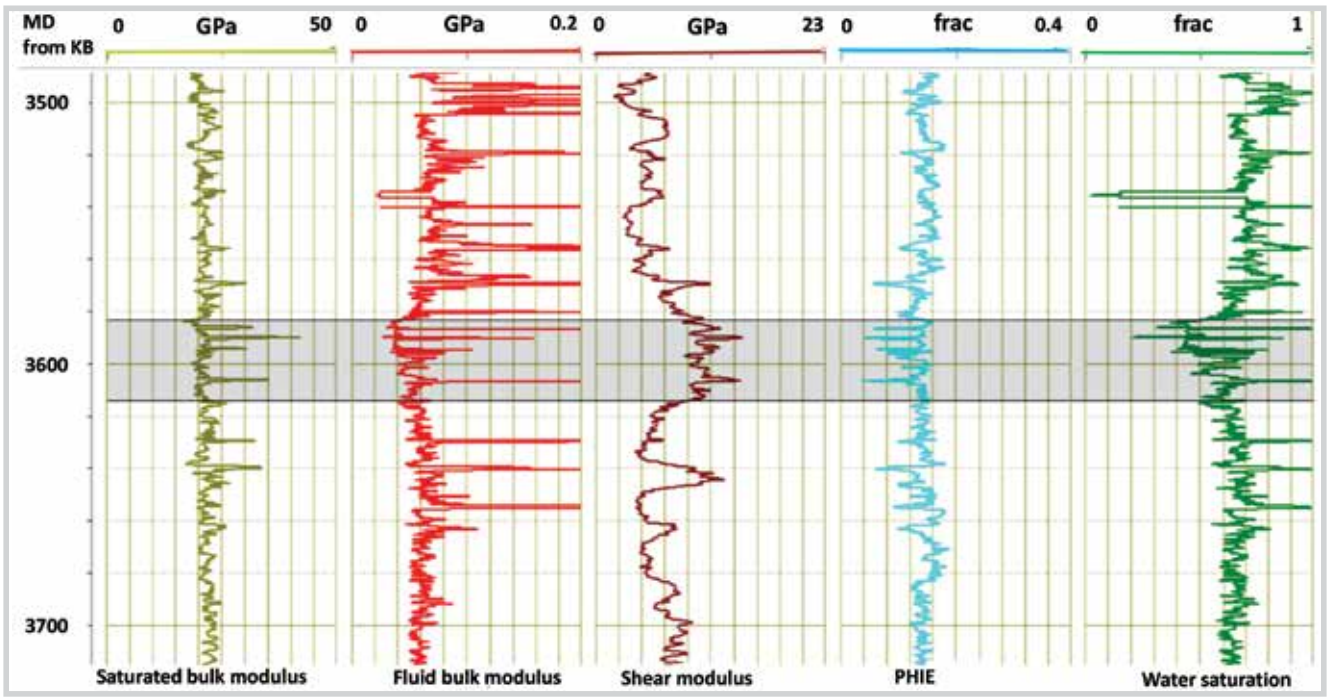

Figure 11. *Well-log based rock physics parameters for calculation of K_d using the modified Gassmann's equation form [22].*

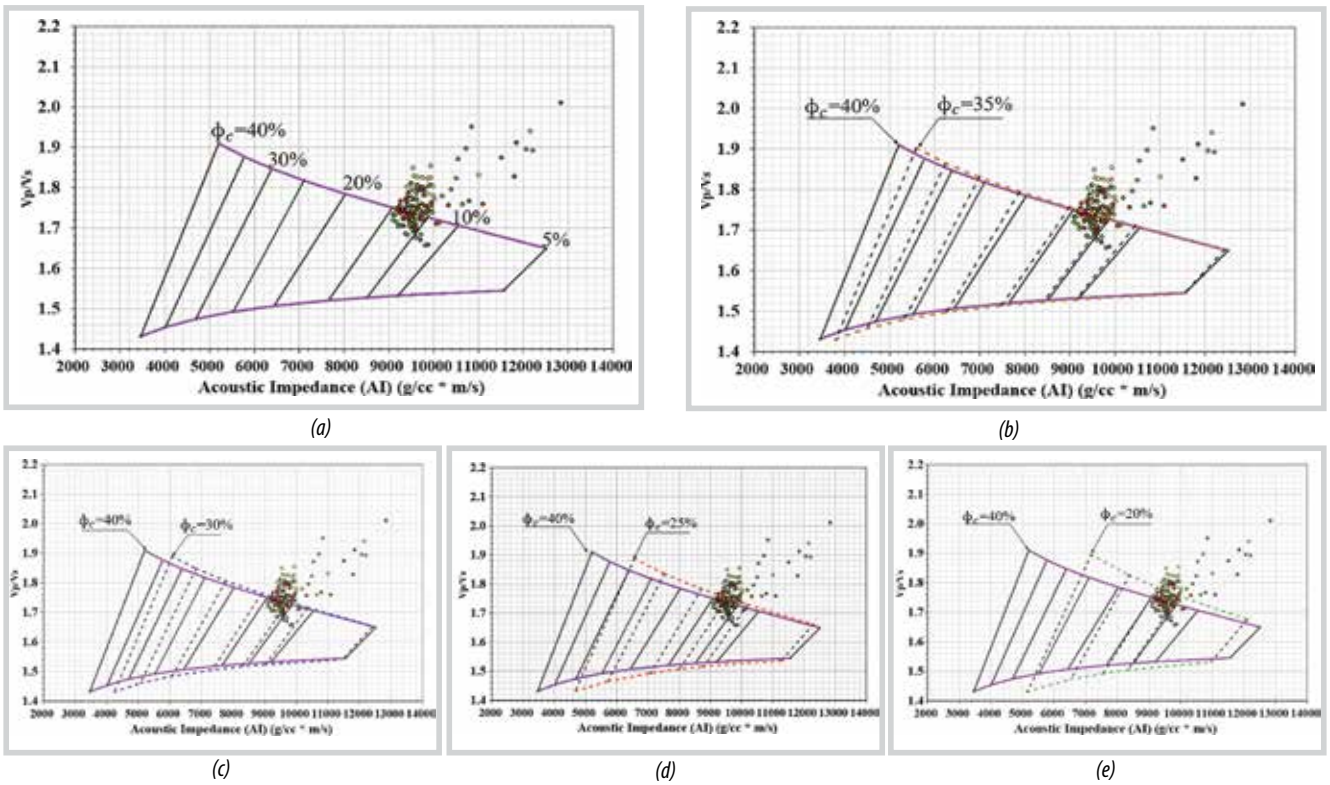

Figure 12. *Effect of change in critical porosity on RPT with ϕ_c = 0.4, 0.35, 0.3, 0.25, 0.20, respectively (Note: green points are of low GR, while yellow points are of high GR).*

g/cc, in addition a crossover between NPHI and RHOB was found. In the study well E2, the MMS reservoir (3,548.57 to 3,584.40m TVDSS) is interpreted having a net pay of 13.39m and moderate reservoir quality with 12% effective porosity, 20% of shale volume and 49% water saturation, respectively. Note that the effective porosity was calculated as the average of NPHI and PHID, and water saturation was estimated by Archie's laws.

In this analysis using Hampson-Russel software the average elastic moduli (K_m and G_m) were calculated using Reuss's lower elastic bound [12] in Equations 1c-d and with fraction of minerals shown in Table 1a. Results of rock physics template construction using Hampson Russel is shown in Figure 10 [23], where one can see that many MMS points lie beyond the 100% gas saturation (Sg = 100%). Thus, this RPT is still not good enough for characterisation of MMS and the answers are suspected to be found in selection of rock physics parameters, the problem that will be addressed in the immediately following section.

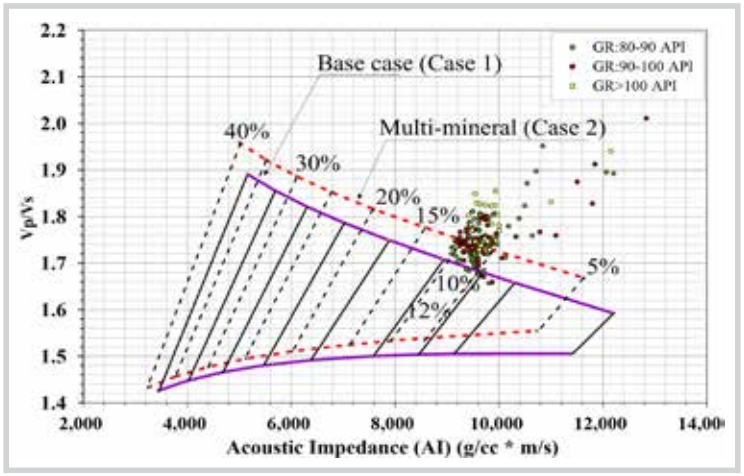

(a)

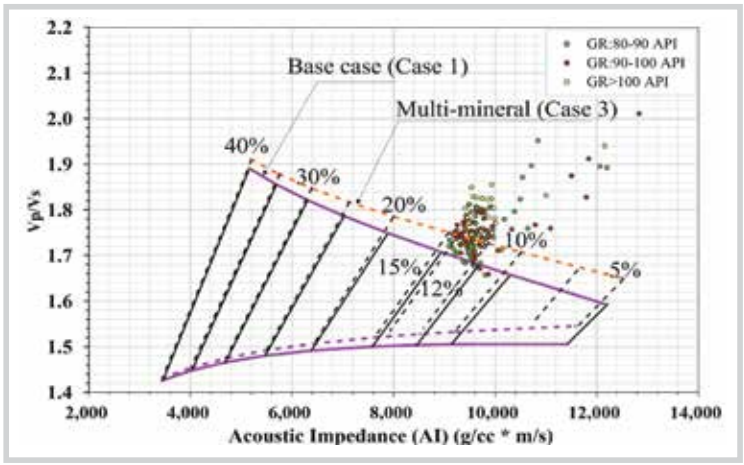

(b)

Figure 13. *Effects of K_m on construction of RPT: (a) case 2 vs. case 1; (b) case 3 vs. case 1.*

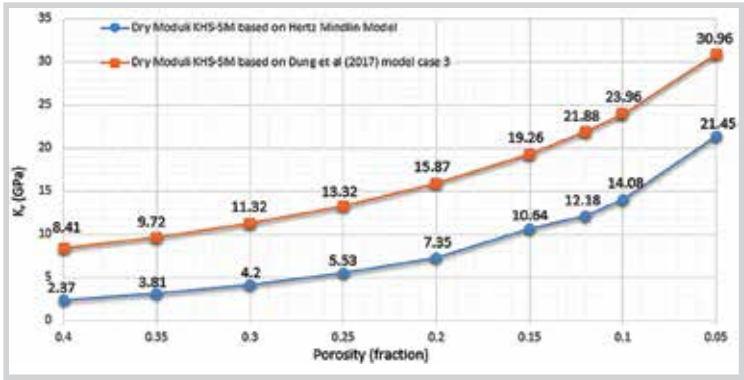

Figure 14. *Comparison of K_d calculated based on Hertz-Mindlin's model [15, 16] and Dung [22].*

5.2. Construction of RPT using a modified approach in this study

Well log analysis for the depth interval from 3,574.5 to 3,614m MD was revisited as shown in Figure 11 and gave the following petrophysical parameters of MMS, and namely: ø = 0.12, K = 21.84GPa, G = 12GPa, K_f = 0.042GPa, and K_d = 21.88GPa where K_d was calculated by modified Gassmann's equation by [21]. After a number of analyses the Voigt-Reuss-Hill's average elastic bound [13] was found to be the best to calculate the mineral moduli (K_m and G_m), which were estimated as 42.43GPa and 38.51GPa, respectively.

5.2.1. Influence of critical porosity (ϕ_c) on RPT construction

Normally for a sand reservoir the critical porosity (ϕ_c) is 40%. As seen in Table 2 this critical porosity can vary for different rock types. To see the effects of critical porosity on the RPT curves a number of charts were constructed for ϕ_c = 40, 35, 30, 25 and 20% as shown in Figure 12. It was observed that the change in critical porosity brings the change in the shape of RPT curves.

5.2.2. Influence of change in bulk and shear mineral moduli

To investigate the influence of the change in bulk and shear of mineral moduli on RPT construction, three cases were compared, and namely: i) case 1 or the base case (with matrix made of Quartz only); case 2 that is the case study by [23]; iii) and case 3 in this study with

mineral fractions based on XRD results as shown in Table 1a. Figure 13a shows that in case 2 with K_m and G_m being estimated by using Reuss's bound [12] the porosity range is from 10 to 12%, while for case 3 that made use of the Voigt-Reuss-Hill's average bound [13] the porosity range is from 12 to 15% as seen in Figure 13b. The latter fits better with the well log analysis results. Thus, the results of XRD analysis are very important in calculating the mineral moduli beside selection of a good elastic bound.

5.2.3. Influence of change in dry bulk modulus of the rock frame (K_d)

Basically, this study found that a change in K_d would shift the RPT curves noticeably. Figure 14 shows a comparison of the dry rock framework moduli (K_d) calculated by Hashin-Shtrikman's model [20] based on Hertz Mindlin's model [15, 16] with those calculated using a modified form of Gassmann's equation as proposed by [22]. The latter method could give a consistently higher K_d as seen in Figure 14. The change in K_d could shift the RPT curves to fit better with well log data points as shown in Figure 15. Finally, a new RPT was successfully constructed for MMS as presented in Figure 16.

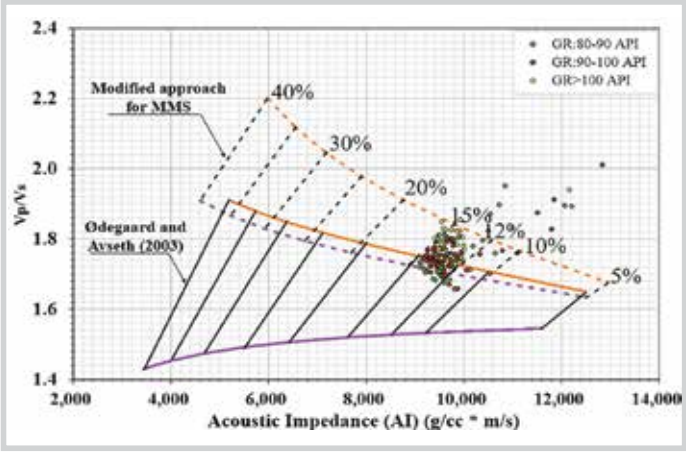

Figure 15. *Influence of K_d on RPT curve shifting.*

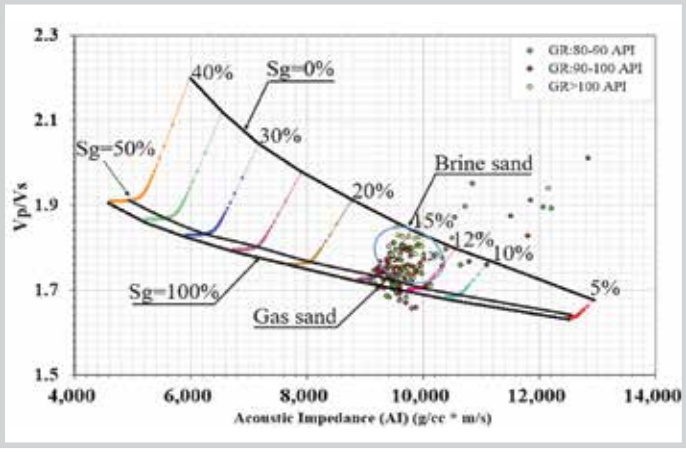

Figure 16. *The RPT constructed in this study for MMS.*

6. Conclusions and recommendations

Based on a detailed parametric analysis in this study it was found that the rock physics parameters such as critical porosity, co-ordination number, mineral fractions, the dry bulk and shear moduli etc. are very important in the construction of RPT for a certain site. Inadequate rock physics parameters could lead to uncertainties in characterisation of clastic reservoir, thus these parameters should be properly tested and estimated, taking into account the site-specific conditions. In this study a new RPT was successfully constructed using the Voigt-Reuss-Hill average elastic bound and a modified form of Gassmann's equation for the gas-bearing Middle Miocene sand at Hai Thach field. As results, the MMS is well characterised with acoustic impedance (AI) from 9,000 to 11,000 m/s×g/cc, and V_p/V_s from 1.65 to 1.80, porosity from 11 to 16%, and gas saturation from 50% up. It is recommended that the RPT construction procedure proposed in this study be applied for other gas-bearing sands in the Nam Con Son basin.

References

1. Pham Huy Giao. *Lithological zoning using the V_p/V_s Log curves*. The 21st Formation Evaluation Symposium of Japan (JFES 2015). Chiba, Japan. 13 - 14 October 2015.

2. Bui Viet Dung, Hoang Anh Tuan, Nguyen Van Kieu, Ha Quang Man, Nguyen Thi Thanh Thuy, Pham Thi Dieu Huyen. *Depositional environment and reservoir quality of Miocene sediments in the central part of the Nam Con Son basin, Southern Vietnam shelf*. Marine and Petroleum Geology. 2018; 97: p. 672 - 689.

3. Phan Trung Dien, Lars Henrick Nielsen, Claus Andersen, Do Van Nhuan. *Late Mesozoic to Cenozoic basin development along the North-West margin of the East Vietnam sea*. American Association of Petroleum Geologists Annual Convention. Salt Lake City, Utah. 1998.

4. C.K.Morley, R.King, R.Hillis, M.Tingay, G.Backe. *Deepwater fold and thrust belt classification, tectonics, structure and hydrocarbon prospectivity: A review*. Earth-Science Reviews. 2011; 104(1-3): p. 41 - 91.

5. Nguyen Quang Tuan, Tran Van Tri. *Seismic interpretation of the Nam Con Son basin and its implica-*

tion for the tectonic evolution. Indonesian Journal on Geoscience. 2016; 3(2): p. 127 - 137.

6. Vietnam Oil and Gas Group. *Petroleum geology and resources of Vietnam*. Science and Technical Publishing House, Hanoi. 2009.

7. Carl Reine. *Discovering a supermodel - A rock - Physics tutorial*. CSEG Recorder. 2017; 42(2): p. 20 - 25.

8. Ødegaard, P.Avseth. *Interpretation of elastic inversion results using rock physics templates*. 65th EAGE Conference & Exhibition. 2003.

9. Jack Dvorkin, Amos Nur. *Elasticity of high-porosity sandstones: Theory for two North Sea datasets*. Geophysics. 1996; 61(5): p. 1363 - 1370.

10. Pham Huy Giao, Pham Hong Trang, Mai Thi Huyen Trang. *Revisit of rock physics template (RPT) construction for petrophysical characterisation of a gas sand in the Nam Con Son basin, Vietnam*. Extended abstract submitted for the 2nd EAGE - VPI Conference on Reservoir Geoscience. Hanoi, Vietnam. 2 - 4 December, 2019.

11. W.Voigt. *Bestimmung der Elastizita¨tskonstanten des brasilianischen Turmalines*. Annual Review of Physical Chemistry. 1890; 41: p. 712 - 729.

12. A.Reuss. *Berechnung der fließgrenze von mischkristallen auf grund der plastizitätsbedingung für einkristalle*. ZAMM-Journal of Applied Mathematics and Mechanics/ Zeitschrift für Angewandte Mathematik und Mechanik. 1929; 9(1): p. 49 - 58.

13. R.Hill. *The elastic behavior of crystalline aggregate.* Proceedings of the Physical Society Section A. 1952; 65(5): p. 349 - 354.

14. Gary Mavko, Tapan Mukerji, Jack Dvorkin. *The rock physics handbook (2nd edition)*. Cambridge University Press. 2009.

15. Raymond David Mindlin. *Compliance of elastic bodies in contact*. Journal of Applied Mechanics. ASME. 1949; 16: p. 259 - 268.

16. Herinrich Hertz. *On the contact of elastic solids.* J. Reine Angew. Math. 1881; 92: p. 156 - 171.

17. William F.Murphy III. *Effects of microstructure and pore fluids on the acoustic properties of granular sedimentary materials*. Stanford University. 1982.

18. Per Avseth, Tapan Mukerji & Gary Mavko. *Quantitative seismic interpretation: Applying rock physics tools to reduce interpretation risk*. Cambridge University Press. 2010.

19. Amos M.Nur, Gary Mavko, Jack Dvorkin, Doron Gal. *Critical porosity: the key to relating physical properties to porosity in rocks*. SEG Technical Program Expanded Abstracts. Society of Exploration Geophysicists. 1995: p. 878 - 881.

20. Z.Hashin, S.Shtrikman. *A variational approach to the theory of the elastic behaviour of multiphase materials.* Journal of the Mechanics and Physics of Solids. 1963; 11(2): p. 127 - 140.

21. Fritz Gassmann. *Über die elastizität poröser medien*. Vierteljahrss-chrift der Naturforschenden Gesellschaft. Zurich. 1951; 96: p. 1 - 23.

22. Tran Trung Dung, Carl H.Sondergeld, Jean-Claude Roegiers. *Different forms of Gassmann equation and implications for the estimation of rock properties*. Petrovietnam Journal. 2017; 10: p. 23 - 29.

23. Mai Thi Huyen Trang. *Application of rock physic template in interpretation of elastic inversion results for the Middle Miocene sand in Nam Con Son basin, Vietnam.* Master Thesis. Asian Institute of Technology. Bangkok, Thailand. 2018.